Available online at www.sciencedirect.com
SCIENCE DIRECT®
Journal of Power Sources 146 (2005) 431–435
JOURNAL OF POWER SOURCES
www.elsevier.com/locate/jpowsour

Electrochemical effect of coating layer on the separator based on PVdF and PE non-woven matrix

Yong Min Lee [a], Nam-Soon Choi [a], Je An Lee [a], Wan-Ho Seol [a], Ki-Yun Cho [a], Ho-Young Jung [a], Jun-Woo Kim [b], Jung-Ki Park [a,*]

[a] *Department of Chemical and Biomolecular Engineering, Korea Advanced Institute of Science and Technology, 373-1, Guseong-dong, Yuseong-gu, Daejeon 305-701, Republic of Korea*
[b] *FinePol Co., 727-2, Sinpyoung-ri, Jijeong-myoun, Wonju-si, Kwangwon-do 220-823, Republic of Korea*

Available online 3 June 2005

Abstract

The coated separator was prepared by coating poly(vinyl acetate) (PVAc) on the surface of the novel separator based on poly(vinylidene fluoride) (PVdF) and polyethylene (PE) non-woven matrix. The ionic conductivity of the coated separator was 1.1×10^{-3} S cm^{-1} at 25 °C, a little higher than that of bare separator. The coated separator showed smoother surface morphology and better adhesion property toward electrodes, and thereby it resulted in lower total resistance than the bare separator. The discharge capacity of the unit cell with coated separator at C/2 rate was maintained at about 84% of the theoretical capacity, which is quite higher than that of the unit cell with the bare separator.

Keywords: Coated separator; Poly(vinyl acetate); Poly(vinylidene fluoride); Polyethylene non-woven matrix; Phase inversion; Rechargeable lithium battery

1. Introduction

The separator is one of the key component materials used for rechargeable lithium batteries. It plays an important role in the ion-conduction and safety behavior in the lithium batteries. The conventional polyethylene separators are not sufficiently compatible with liquid electrolyte, and thus there have been many efforts on modification of the surface of the separator to enhance the compatibility [1–6]. In addition, there were also some studies on the cost-reduction of the separator by using non-polyolefin polymers [7,8]. Use of polyethylene (PE) non-woven matrix is one of the ideas to reduce the manufacturing cost of separator while maintaining the mechanical strength and thermal shutdown property of the polyethylene separator. Our group has already reported the novel separator system based on poly(vinylidene fluoride) (PVdF) and PE non-woven matrix [9]. However, it is still required to modify the surface of the separator due to the rough surface morphology. In this work, we tried to properly coat the surface of the separator in order to enhance the electrochemical performance of the unit cell.

2. Experimental

2.1. Preparation of PVAc-coated separators based on PVdF and PE non-woven matrix

The novel porous separator (bare separator) based on PVdF (M_w = 600,000, Solvay) and PE non-woven matrix was prepared by coating the PVdF/NMP solution upon the PE non-woven matrix [9]. An appropriate amount of poly(vinyl acetate) (PVAc, M_w = 500,000, Aldrich), a coating material, was dissolved in an anhydrous acetone. The separator was then immersed in the polymer solution. The separator was taken out and left to evaporate the solvent at room temperature. After evaporation of the solvent, it was under vacuum at 40 °C for 12 h to remove the residual solvent and water trace.

* Corresponding author. Tel.: +82 42 869 3925; fax: +82 42 869 3910.
E-mail address: jungpark@kaist.ac.kr (J.-K. Park).

0378-7753/$ – see front matter © 2005 Elsevier B.V. All rights reserved.
doi:10.1016/j.jpowsour.2005.03.047

2.2. Measurement of physical properties of the coated separator

The specimens for the SEM images of the cross-section of the separator were prepared by fracturing the corresponding film in liquid nitrogen. The pore size distribution and porosity of separator were measured with mercury porosimeter.

Thermal behavior of the separator was studied by using a differential scanning calorimeter. It was scanned from −80 to 200 °C by heating at a rate of 10 °C min^{-1} under nitrogen atmosphere.

2.3. Preparation of electrodes

The anode has a composition of 95 wt% graphitized mesocarbon microbeads (MCMB2528) and 5 wt% Kynar 741 as a binder material. The cathode is composed of 88 wt% $LiCoO_2$, 6.8 wt% super-P and 5.2 wt% Kynar 741. The loading density of active material corresponded to a capacity of 2.4 mAh cm^{-2}. Both the cathode and the anode were immersed into liquid electrolyte before cell assembly to fill the pores in the electrodes with the liquid electrolyte.

2.4. Electrical measurements

The separator dipped in liquid electrolyte, 1 M $LiPF_6$ in ethylene carbonate(EC)/diethyl cabonate(DEC)/propylene carbonate(PC)[35/60/5, w/w/w] (Samsung Cheil Industries, Korea), was sandwiched between the two stainless steel (SS) electrodes to measure the ionic conductivity. The ionic conductivity was obtained from bulk resistance measured by ac complex impedance analysis using a Solartron 1255

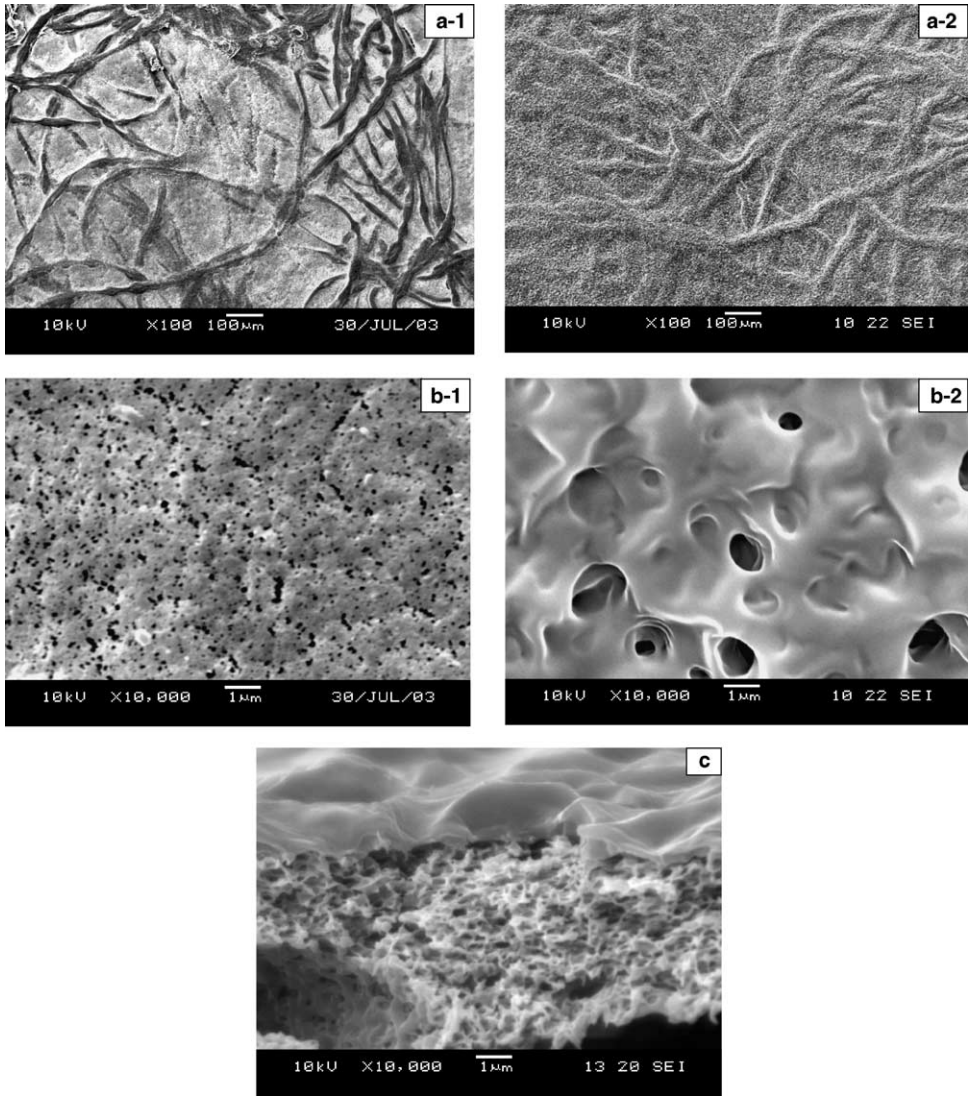

Fig. 1. Scanning electron micrographs of the bare and coated separators (a) surface morphology(×100) of bare[a-1] and coated[a-2] separators; (b) magnified surface morphology(×10,000) of bare[b-1] and coated[b-2] separators; (c) coating layer morphology(×10,000) upon the porous PVdF layer; (d) cross-section morphology of bare[d-1] (×2500) and coated[d-2] (×2000) separators and (e) magnified cross-section morphology of bare[e-1] (×15,000) and coated[e-2] (×10,000) separators.

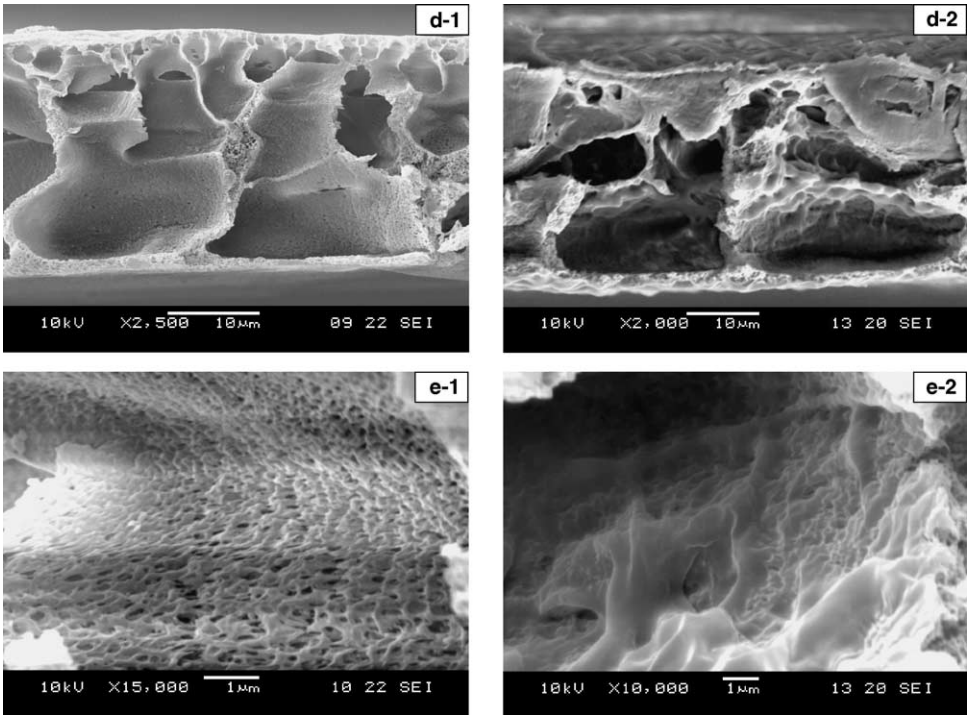

Fig. 1. (*Continued*).

frequency response analyzer (FRA) over frequency range of 100 Hz–1 MHz.

The unit cell was assembled by sandwiching the separator after soaking it in the liquid electrolyte between carbon anode and $LiCoO_2$ cathode. The cell (2 cm × 2 cm) was then sealed in an aluminized polyethylene bag. The unit cell was typically cycled between 2.7 and 4.2 V at a constant current density at room temperature using a TOSCAT-3000U (Toyo System Co., Ltd.). The charge process was cut-off at 20% of the initial constant current.

3. Results and discussion

3.1. Physical properties of the coated separator

Fig. 1(a and b) present scanning electron micrographs of the surface of the bare and coated separators. It is clearly observed that the surface of the coated separator is much smoother than that of the bare separator. Thin coating layer was formed upon porous PVdF phase as shown in Fig. 1(c). From the cross-sectional image shown in Fig. 1(d and e), it is found that the inside of macropore in the separator is also coated with PVAc owing to the hydrophilic property of PVdF. This is not usually observed in the coated separator based on polyolefin separator [3]. As a result, the porosity decreased to 48% and the average pore size was also decreased to 32 nm as shown in Table 1. The internal morphology of the coated separator became less porous as compared to that of the bare separator.

3.2. Thermal properties of the coated separator

PE non-woven matrix is also expected to provide the coated separator with thermal shutdown property. Fig. 2 shows the DSC thermograms of the bare separator, coating material (PVAc) and coated separator. The melting temperature and crystallinity of PE non-woven matrix phase in the

Table 1
The properties of bare and coated separators

Property	Bare separator	Coated separator
Thickness (dry condition) (μm)	33 ± 1	37 ± 1
Thickness (after soaked with liquid electrolyte) (μm)	40 ± 1	38 ± 1
Porosity (%)	53	48
Average pore size (nm)	35	32
Uptake amount[a] (%)	290	302
Ionic conductivity at 25 °C (S cm^{-1})	8.9×10^{-4}	1.1×10^{-3}

[a] The uptake amount into the porous phase in the separator, uptake amount (%) = $(W - W_0)/W_0 \times 100$, where W and W_0 are the weights of the wet and dried separator, respectively.

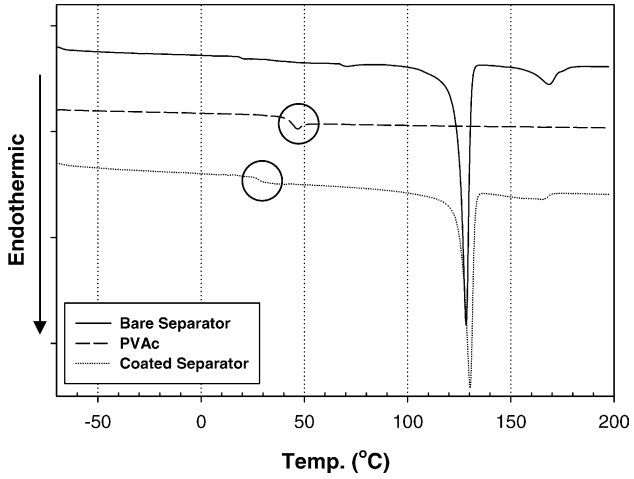

Fig. 2. DSC thermograms of the bare separator, coating material [PVAc] and coated separator.

coated separator was kept almost unchanged, which can lead to a proper thermal shutdown operation of the cell. However, the crystallinity of PVdF phase in the coated separator was reduced to 75% of the crystallinity of PVdF in the bare separator and the glass transition temperature (T_g) of PVAc decreased from 45 to 30 °C. They resulted from the penetration of PVAc into PVdF phase during the coating process.

3.3. Ion conductivity of the coated separator and its dimensional stability

The ionic conductivity of the coated separator was 1.1×10^{-3} S cm^{-1} at 25 °C, a little higher than that of bare separator (8.9×10^{-4} S cm^{-1}) as shown in Table 1. It is thought that the enhancement of the ionic conductivity of the coated separator comes from a little higher uptake amount of the liquid electrolyte (EC/DEC/PC=35/60/5, wt ratio).

It is found that the coating layer plays an important role of maintaining the dimensional stability of the coated separator. In the case of the bare separator, its thickness increased about 20% (7 μm) after soaking in the liquid electrolyte, which

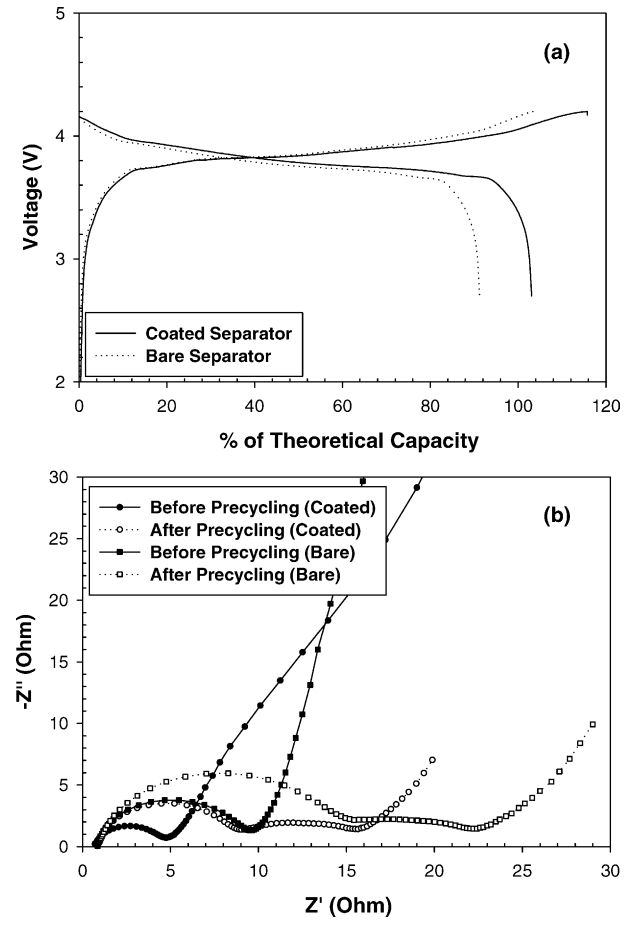

Fig. 3. (a) Preconditioning charge/discharge curves of the unit cell of carbon/(bare or coated separator)/$LiCoO_2$ at room temperature (current density = 0.24 mA cm^{-2} (C/10 rate) and cut-off voltage = 2.7–4.2 V) and (b) the ac impedance spectra of the unit cell before and after preconditioning cycle.

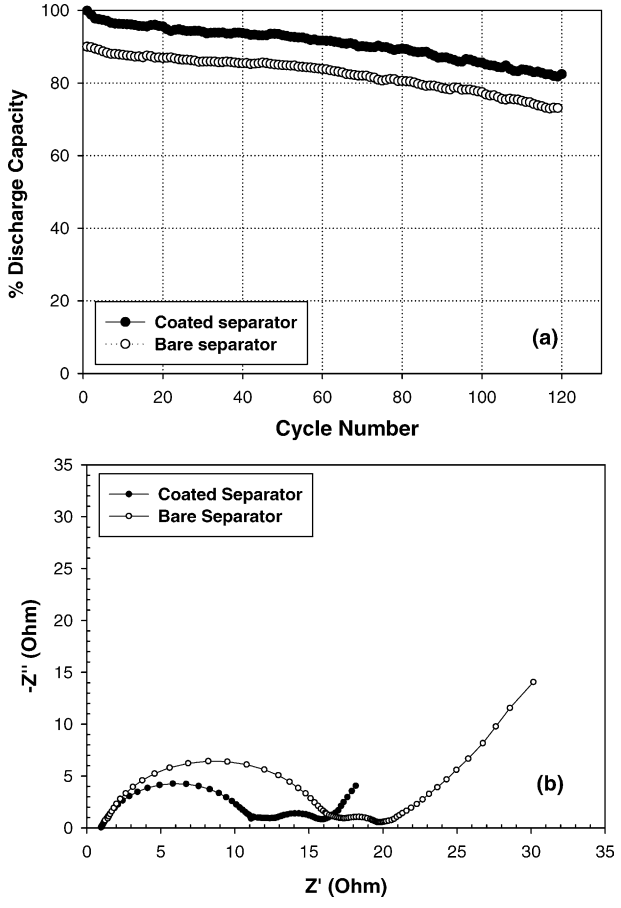

Fig. 4. (a) Charge/discharge capacity as a function of cycle number of the unit cell of carbon/(bare or coated separator)/$LiCoO_2$ at room temperature at C/2 (1.2 mA cm^{-2}) rate (liquid electrolyte, 1 M $LiPF_6$ in EC/DEC/PC = 35/60/5, w/w/w) and (b) the ac impedance spectra of the unit cells after 120 cycles.

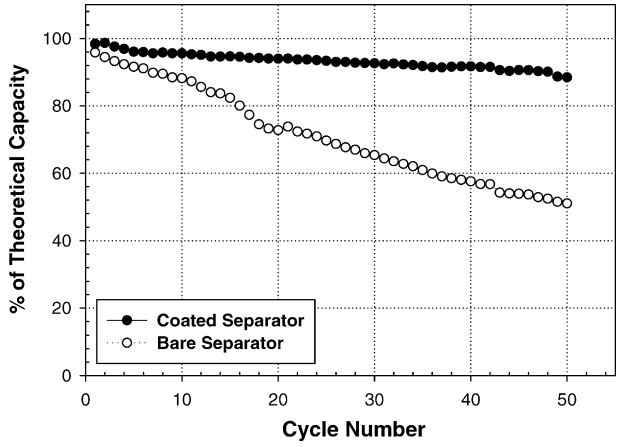

Fig. 5. Charge/discharge capacity as a function of cycle number of the unit cell of carbon/(bare or coated separator)/$LiCoO_2$ at room temperature at 1C (2.4 mA cm^{-2}) rate.

results from the poor compatibility between PVdF and PE non-woven matrix. However, the thickness of the coated separator was maintained within only 1 μm even after soaking in the liquid electrolyte.

3.4. Electrochemical performance of the coated separator

The assembled unit cells were subjected to a preconditioning cycle with cut-off voltages of 4.2 V for the upper limit and 2.7 V for the lower limit at a constant current of 0.24 mA cm^{-2} (C/10 rate) before the repeated charge and discharge at higher rate. Fig. 3(a) represents the charge/discharge profile for the preconditioning cycle. The discharge capacity for the preconditioning cycle of the unit cell with coated separator is about 100% of the theoretical capacity and the coulombic efficiency (charge/discharge efficiency) is about 89%. This higher discharge capacity for the preconditioning cycle as compared to the unit cell with bare separator is mainly due to the lower total resistance as shown in Fig. 3(b), which may result from smoother surface morphology and better adhesion property of PVAc towards the electrodes. Fig. 4(a) shows the charge and discharge capacity of the two different unit cells as a function of cycle number at C/2 rate. The discharge capacity of the unit cell based on the coated separator is higher, which is 84% of the theoretical capacity for 120th cycle. This is much due to the lower total resistance of the unit cell based on the coated separator as is seen in Fig. 4(b).

Fig. 5 shows discharge capacity of the unit cells as a function of cycle number at higher (1C) rate with CC/CV charge condition. The unit cell with the coated separator shows also much higher discharge capacity than that with bare separator in the high rate. It suggests that the coating layer is very critical in determining the cyclability at higher current rate.

4. Conclusions

PVAc was successfully introduced as a coating material on the surface of the novel porous separator based on PVdF and PE non-woven matrix. The coated separator showed smoother surface morphology and better adhesion property toward electrodes, which could lead to a lower total resistance. The cell performance was much improved by coating of the separator with a proper material as compared to the bare separator.

Acknowledgement

This work was supported by the Ministry of Commerce, Industry and Energy in Korea.

References

[1] K. Morigaki, N. Kabuto, K. Haraguchi, Matsushita Electric Industrial, US Patent 55,976,59, issued January 28, 1997.
[2] K.M. Abraham, M. Alamgir, D.K. Hoffman, J. Electrochem. Soc. 142 (1995) 683–687.
[3] D.-W. Kim, J.-M. Ko, J.-H. Chun, S.-H. Kim, J.-K. Park, Electrochem. Commun. 3 (2001) 535–538.
[4] D.-W. Kim, K.A. Noh, J.-H. Chun, S.-H. Kim, J.-M. Ko, Solid State Ionics 144 (2001) 329–337.
[5] D.-W. Kim, B. Oh, J.-H. Park, Y.-K. Sun, Solid State Ionics 138 (2000) 41–49.
[6] Y. Wang, J. Travas-Sejdic, R. Steiner, Solid State Ionics 148 (2002) 443–449.
[7] I. Kuribayashi, J. Power Sources 63 (1996) 87–91.
[8] P.P. Prosini, P. Villano, M. Carewska, Electrochim. Acta 48 (2002) 227–233.
[9] Y.M. Lee, J.W. Kim, N.-S. Choi, J.A. Lee, W.-H. Seol, J.-K. Park, J. Power Sources 139 (1–2) (2005) 235–241.